Traceable long-range wide-area network workflow for hydroclimatic and soil monitoring in tropical agriculture

Flujo trazable con LoRaWAN para monitoreo hidroclimático y edáfico en agricultura tropical

Yulieth Carriazo-Regino[1, 2], Rubén Baena-Navarro[1, 2, 3 *], Mario Macea-Anaya[1]

1 Department of Systems and Telecommunications Engineering, Faculty of Engineering, Universidad de Córdoba. Montería, Colombia.
2 Doctorate Program in Informatics (Computer Science), Postgraduate Division, Universidad Americana de Europa. Cancún, Mexico.
3 Systems Engineering Program, Faculty of Engineering, Universidad Cooperativa de Colombia. Montería, Colombia.

SOUTH SUSTAINABILITY

Cite as: Carriazo-Regino, Y. *et al.* (2026). «Traceable long-range wide-area network workflow for hydroclimatic and soil monitoring in tropical agriculture». *South Sustainability*, 7(2). DOI:10.21142/SS-0702-2026-e178

Received: 7/7/2026
Peer reviewed
Accepted: 30/10/2026

© Los autores, 2026. Publicado por la Universidad Científica del Sur (Lima, Perú)

* Corresponding author:
rbaena@correo.unicordoba.edu.co

Associate editor:
Thomas Marambanyika

ABSTRACT

In this study, we present a traceable long-range wide-area network (LoRaWAN) workflow for tropical agricultural monitoring. The method employed integrated an expected hourly calendar, local storage, delivery states, calibration metadata and quality-control rules. A computational demonstration used estimated and completed 2025 series associated with Montería, Colombia. Of a total of 8760 scheduled records, 8322 were marked received (95.0%); 438 absences formed 411 episodes, including 386 single-record episodes. Monthly mean battery voltage decreased from 4.175 to 3.823 V, with a minimum of 3.731 V. The workflow quantifies discontinuity and preserves data origin across processing stages. The results of the study characterize the computational series and illustrate traceable reporting of telemetry and energy indicators.

Keywords: *agricultural IoT, LoRaWAN, soil moisture, hydroclimatic monitoring, telemetry traceability, data quality control*

RESUMEN

Se presenta un flujo trazable de red de área amplia y largo alcance (LoRaWAN) para monitoreo agrícola tropical. El método integra un calendario horario, almacenamiento local, estados de recepción, metadatos de calibración y reglas de calidad. Una demostración computacional utiliza series estimadas y completadas de 2025 asociadas con Montería (Colombia). De 8760 registros programados, 8322 figuran recibidos (95,0 %); las 438 ausencias forman 411 episodios, incluidos 386 de un registro. El voltaje medio mensual disminuye de 4,175 a 3,823 V, con mínimo de 3,731 V. El flujo cuantifica discontinuidades y conserva la procedencia durante el procesamiento. Los resultados caracterizan las series computacionales e ilustran la presentación trazable de indicadores de telemetría y energía.

Palabras clave: *IoT agrícola, LoRaWAN, humedad del suelo, monitoreo hidroclimático, trazabilidad de telemetría, control de calidad de datos*

1. Introduction

Increasingly, agricultural water monitoring combines local weather, soil-water sensing and low-power communication factors, because root-zone conditions can diverge from regional products at field scale. In the context of tropical production, additional factors include intense rainfall, high humidity and rapid wetting–drying transitions, which can complicate sensor interpretation (Dhanaraju *et al.*, 2022; Obaideen *et al.*, 2022; Nsoh *et al.*, 2024; Loconsole *et al.*, 2025). Therefore, reliable monitoring requires evidence of both the environmental state and system operation. For example, a change in soil moisture must be interpreted alongside the continuity and quality of the data record.

Internet of Things (IoT) systems connect sensors to local storage and remote services, making observations accessible between field visits (García *et al.*, 2020). The LoRaWAN protocol provides long-range, low-data-rate communication suited to sending small agricultural measurements. Its usefulness is contingent upon the complete measurement and communication path, including sensor calibration, reception and power supply (Aldhaheri *et al.*, 2025). Published applications include irrigation monitoring in tomatoes, soil-nitrate sensing, and soil-water monitoring in woody crops (Zhang *et al.*, 2022; Bristow *et al.*, 2022; Dafonte *et al.*, 2024). These examples establish practical uses while also demonstrating why the measured variable and the system's operating conditions must be reported together.

At an international level, experiments have illustrated the environmental dependence of these systems. Orchard tests in Korea have examined the effect of vegetation on a 915 MHz LoRa link, and maize experiments in China have investigated how antenna height influences propagation at 433 MHz (Ahmed *et al.*, 2025; Xu *et al.*, 2025). Solar-assisted viticulture monitoring has considered delivery alongside the energy budget and acquisition schedule (Vieira *et al.*, 2026). Furthermore, agricultural communication studies have addressed packet loss, rural connectivity and changing environmental conditions (Dai *et al.*, 2024; Chapungo and Postolache, 2025; Alkhayyal and Mostafa, 2025). Together, these studies explain why a delivery percentage requires an explicit evaluation period and operating context.

In Latin America, a Chilean LoRa platform connects agricultural measurements to remote monitoring services (Ahmed *et al.*, 2022). In Colombia, the Digital Agroclimatic Plot in Palmira combines soil and climate sensors, LoRaWAN communication and visualization (Barrios *et al.*, 2025). These initiatives provide regional examples of how sensing and connectivity can support agricultural observation. The application of their approaches at another site would involve more than the transferring of hardware; the acquisition schedule, soil conditions, local storage and reception record determine the information that is available for interpretation.

Montería provides a relevant tropical agricultural context because seasonal rainfall and humid vegetation can affect both soil-water dynamics and the communication path. Regional soil research and agricultural planning describe the setting, but do not establish the properties of each individual plot (Cadena-Torres *et al.*, 2021; *Unidad de Planificación Rural Agropecuaria*, 2025). Furthermore, soil-moisture readings are dependent upon the characteristics of the soil, probe installation and calibration (Mane *et al.*, 2024; Abdelmoneim *et al.*, 2025; Raheja *et al.*, 2025). During rapid wetting or drying, an incomplete sequence can conceal when a soil response began. Therefore, the problems associated with local monitoring include both environmental variation and the ability to retain a usable record of such variation.

Modular farm architectures and irrigation testbeds integrate sensing with communication and remote services (Codeluppi *et al.*, 2020; Froiz-Míguez *et al.*, 2020). In order to compare and interpret their records, a link is required between expected observations, locally retained readings, remote delivery, energy state, calibration history, field events and quality-control decisions. These elements illustrate different aspects of the same monitoring process. For example, a reading stored locally, while absent remotely, indicates a different information gap from a scheduled observation with no acquisition record. A complete account preserves that distinction throughout the analysis.

The methodological gap addressed in this study is how to retain those relationships within one reproducible workflow. The exclusion of missing transmissions from the expected calendar can inflate apparent completeness and obscure interruptions in the environmental record. Furthermore, an annual availability percentage cannot distinguish predominantly isolated gaps from prolonged gaps. The preserving of each scheduled timestamp, its data origin and its reception state enables the evaluating together of completeness and the temporal distribution of losses. Calibration and event metadata then provide context for interpretation of the values that remain available.

The goal was to define a traceable LoRaWAN workflow for tropical agricultural monitoring. The method describes an end-to-end acquisition and storage architecture with calibration and quality control, characterizing a full year of hydroclimatic, soil-moisture, telemetry and battery series, and comparing its functions with agricultural systems and scientific loggers. A computational demonstration was conducted using both estimated and completed 2025 data series associated with Montería. The primary contribution of this work lies in the establishing of an explicit connection between environmental records and operational evidence across processing stages. Furthermore, related work by

DOI: 10.21142/SS-0702-2026-e178

the authors provides context in IoT instrumentation, interpretable computational methods and sustainability-oriented assessment (Baena-Navarro *et al.*, 2020, 2024, 2026; Vidal-Durango *et al.*, 2024; Pinedo-López *et al.*, 2025).

2. Study context and workflow design

The demonstration used estimated weather series and computationally completed monitoring records associated with Montería, Colombia (8.74798° N, 75.88143° W). The coordinates provided a geographic reference for the context. The 2025 calendar contained 8760 scheduled hourly records in Colombian local time. Figure 1 summarizes the end-to-end monitoring architecture, separating local measurement and backup from LoRaWAN transmission, remote reception and analytical integration.

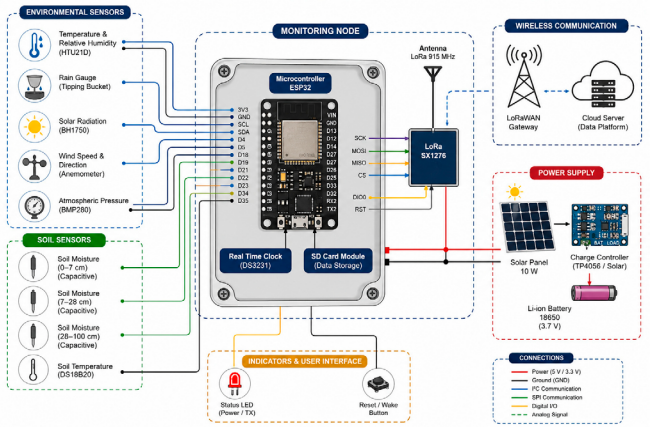


Figure 1. End-to-end monitoring architecture and traceability workflow

Note. Local microSD retention and remote reception are represented as distinct paths. ET0 denotes FAO-56 reference evapotranspiration. The BH1750 channel measures ambient illuminance and is not intended as a substitute for the shortwave-radiation input. RSSI denotes received signal strength indicator; SNR, signal-to-noise ratio. The architecture describes the proposed design; the analysis uses the series identified in Section 2.

Table 1 details the study context, instrumentation, interfaces and roles of the monitoring components.

Table 2 formalizes hourly traceability by retaining every expected timestamp, including positions without remote delivery.

Table 2. Algorithm 1. Traceable hourly record processing and quality control

Step	Operation
Input	Expected hourly calendar; environmental readings; acquisition/reception metadata; calibration pairs; events and quality rules.
1	Match records to their expected timestamp; retain the complete calendar and flag duplicates.
2	Preserve supplied values and their origin; identify estimated or completed records separately from original acquisition records.
3	Retain each missing remote record; distinguish local acquisition from remote delivery where both records are available. Calculate latency for received records only.
4	Attach calibration and event context; apply range, temporal and consistency rules while preserving quality status.
5	Group consecutive missing hourly samples into episodes; calculate daily and monthly summaries with explicit denominators.
Output	Traceable hourly calendar, availability and episode distribution, and eligible environmental and battery summaries. Missing delivery states are retained when calculating availability.

Table 1. Study setting, instrumentation and operational configuration of the monitoring workflow

Layer	Device or variable	Specification / configuration	Role in the workflow
Study setting	Montería agricultural context	2025; hourly series	Site context
hydroclimate	Estimated weather series	Air temperature, RH/dew point, precipitation, wind, shortwave radiation and pressure	FAO-56 and hydroclimatic context
Environment	HTU21D	0–100% RH (±2% typical at 20–80%); −40–125 °C (±0.3 °C typical at 5–60 °C); I2C	Air temperature/humidity
Environment	Tipping-bucket rain gauge; anemometer/wind vane	Dedicated digital/analog inputs; product models unspecified	Precipitation; wind speed/direction
Environment	BH1750; BMP280	Illuminance; pressure 300–1100 hPa (±1 hPa typical at 950–1050 hPa, 0–40 °C); I2C	Light and pressure
Soil	Capacitive-probe design; reported moisture layers	0–7, 7–28 and 28–100 cm series; analog input; soil-specific calibration required	Depth-resolved moisture
Soil	20 cm moisture channel; DS18B20	VWC%; DS18B20 −55–125 °C (±0.5 °C at −10–85 °C); analog/1-Wire	20 cm moisture and soil temperature
Acquisition	ESP32; DS3231; microSD	60 min schedule; I2C timekeeping; SPI local backup	Acquisition, timestamping and local retention
Communication	SX1276; LoRaWAN gateway	915 MHz; SPI radio; delivery, RSSI, SNR and latency indicators	Remote reception and link metadata
Power	Solar panel; charge controller; 18650 Li-ion cell	10 W panel; 3.7 V nominal cell	Power supply and battery-voltage tracking
Protection	Enclosure	Design component; no certified rating	Physical protection

Note. HTU21D, BMP280 and DS18B20 ranges and stated accuracies follow the manufacturer specifications and conditions of use (TE Connectivity, 2017; Bosch Sensortec, 2021; Analog Devices, 2019). RH: relative humidity; VWC: volumetric water content; I2C: inter-integrated circuit; SPI: serial peripheral interface. Components describe the proposed design.

3. Indicator computation and quality control

Reference evapotranspiration ET_0 was retained as supplied with the estimated weather series. Weather inputs and the soil-node channels were treated separately: BH1750 illuminance was not substituted for shortwave radiation. Equation (1) gives the daily Food and Agriculture Organization (FAO)-56 relation used to describe the indicator (Allen *et al*., 1998).

$$ET_0 = \frac{0.408\Delta(R_n - G) + \gamma \frac{900}{T + 273} u_2 (e_s - e_a)}{\Delta + \gamma (1 + 0.34u_2)} \quad (1)$$

Δ is the saturation-vapor-pressure slope and γ the psychrometric constant (kPa °C^{-1}); R_n and G are net radiation and soil heat flux (MJ m^{-2} d^{-1}). T is temperature (°C), u_2 wind at 2 m (m s^{-1}), e_s saturation and e_a actual vapor pressure (kPa). For 10 m wind stored in km h^{-1}, u_2 = 0.207764 u_{10}. Equation (1) is daily.

Equation (2) defines B_d from daily precipitation P_d minus $ET_{0,d}$ (mm), without a soil-water storage balance.

$$B_d = P_d - ET_{0,d} \quad (2)$$

Equation (3) defines availability A (%) from received $N_{received}$ and scheduled $N_{expected}$ records; annually, $N_{expected}$ = 8760.

$$A = \frac{N_{received}}{N_{expected}} \times 100 \quad (3)$$

Equations (4) and (5) define linear checks and absolute errors for sensor type s and pair i: $x_{i,s}$ is raw value, $\beta_{1,s}$ slope, $\beta_{0,s}$ intercept, $y_{i,s}^{lin}$ linear check, $y_{i,s}^{cal}$ stored calibrated value, $y_{i,s}^{ref}$ reference, and $e_{i,s}$ absolute error.

$$y_{i,s}^{lin} = \beta_{1,s} x_{i,s} + \beta_{0,s} \quad (4)$$

$$e_{i,s} = |y_{i,s}^{cal} - y_{i,s}^{ref}| \quad (5)$$

Table 3 summarizes hydroclimatic inputs, traceability, calibration examples, event records and quality-control criteria for the 2025 demonstration.

4. Results

4.1. Hydroclimatic and soil series

Total precipitation was 1781.7 mm, while reference evapotranspiration (ET_0) reached 1333.9 mm. The difference, calculated before rounding, was +447.9 mm; ET_0 exceeded rainfall on 235 days. Hourly water content at a depth of 20 cm ranged from 16.27% to 44.14%; monthly means ranged from 18.48% to 41.04%.

4.2. Telemetry continuity

The 438 missing records formed 411 episodes: 386 contain one record; 23 contain two records; and two contain three records. Single-record episodes account for 93.9% of the total. Mean latency for received records was 1.44 s.

4.3. Battery profile

The monthly mean voltage fell from 4.175 to 3.823 V; the minimum was 3.731 V. Figure 2 aligns these series.

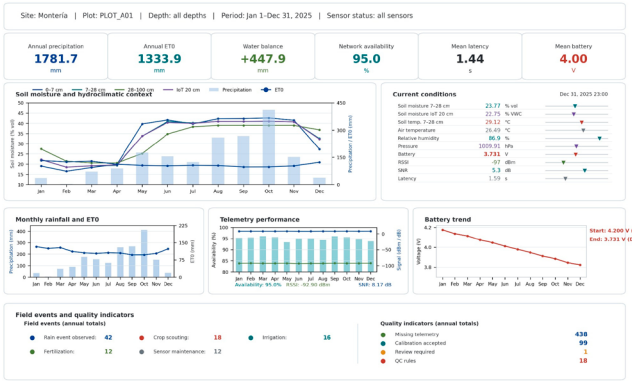


Figure 2. Hydroclimatic, soil-moisture, telemetry and battery-voltage patterns in the 2025 series

Note. (A) Monthly precipitation (P), reference evapotranspiration (ET0) and mean soil water content; the 20 cm series is expressed as m3 m−3 after dividing percentages by 100. (B) Missed hourly transmissions and monthly availability; the dashed line shows annual availability of 95.0%. (C) The 411 episodes contain all 438 missed transmissions; episode length counts consecutive missed scheduled samples, not exact outage duration. (D) Monthly mean battery voltage and minimum–maximum range; shading represents extrema, not confidence intervals. QC denotes quality control: the 3.0 and 4.2 V lines are data-quality limits, not hardware operating thresholds. Estimated and computationally completed series illustrate the workflow; monthly summaries do not establish physical causes or multi-year autonomy.

Table 3. Hydroclimatic inputs, traceability, calibration and quality control in the 2025 demonstration

Component	Entries	Calculation or rule	Result
Hydroclimatic inputs	Estimated weather series; supplied FAO-56 product	Daily ET0 and precipitation totals; BH1750 excluded as radiation source	ET0 1333.9 mm; precipitation 1781.7 mm
Calendar	8760 hourly slots	Received/scheduled	8322/8760; 95.0%
Calibration examples	20 pairs/type; 100 labeled accepted	Mean absolute error	VWC 0.662 pp; T 0.181 °C; pH 0.109; battery 0.0137 V; latency 0.131 s
Events	100 entries	Activity log	42 rain; 18 scouting; 16 irrigation; 12 maintenance; 12 fertilization
Quality control	18 range, temporal and consistency rules	RH/VWC 0–100%; battery 3.0–4.2 V; received latency 0–5 s	One received latency exceeds 5 s; battery QC limits are not operating thresholds

Note. QC: quality control; pp: percentage points. Availability uses the full expected calendar and retains missing delivery states. Calibration pairs illustrate absolute-error calculations rather than independently measured field accuracy (World Meteorological Organization, 2018). Weather estimates, completed records and event entries describe the supplied demonstration series.

DOI: 10.21142/SS-0702-2026-e178

5. Discussion

5.1. Hydroclimatic and soil interpretation

The annual excess of precipitation over reference evapotranspiration, +447.9 mm, coexists with 235 days during which ET_0 exceeded rainfall. This combination illustrates why an annual total can conceal intervals with little rainfall relative to atmospheric demand. The daily difference helps identify those intervals, but it does not directly measure crop water stress or irrigation requirements. In the FAO-56 framework, ET_0 describes a reference surface; interpreting crop demand also involves crop development and soil-water availability (Allen *et al*., 1998).

The 20 cm soil data series provides information at a different scale. With a volumetric water content range of 16.27–44.14%, it captures variation at the reported depth, whereas monthly means summarize slower changes. Neither the lowest value nor the highest value alone define plant stress, field capacity or waterlogging. Those interpretations are dependent upon soil properties, rooting depth and calibration. This aligns with Dafonte *et al*. (2024), who placed soil-sensor interpretation within a calibrated monitoring system for woody crops. In this study, the calibration examples demonstrate the error calculations, as shown in Table 2.

Reading these indicators together clarifies the agricultural purpose of the workflow. Rainfall and atmospheric demand provide context for interpreting changes in soil moisture, while the reception status shows where the sequence is incomplete; a missing transmission during a wetting or drying interval can conceal the timing of the soil response. Keeping the expected calendar and the missing positions visible helps readers assess the information available for that interpretation. The present estimated and completed data series demonstrate this procedure, without establishing a crop response or an irrigation benefit.

5.2. Loss structure and crop canopies

The 95.0% annual availability becomes more informative when considered alongside the distribution of missing records. Of the 411 episodes, 386 contain a single scheduled record, representing 93.9% of all episodes. The missing positions are therefore predominantly isolated at the hourly sampling scale. Networks with the same annual availability can have different practical consequences if one has scattered gaps and another has prolonged gaps. The episode distribution preserves this distinction, which would be concealed by a single annual percentage.

Crop canopies provide a physical context for interpreting such patterns in field networks. Vegetation obstructs and attenuates the radio path, and changes in leaf wetness, leaf position and reflected signal paths can alter reception temporarily. Ahmed *et al*. (2025) examined vegetation effects in a 915 MHz orchard system; Xu *et al*. (2025) have shown the influence of antenna height and crop obstruction in 433 MHz maize trials. These studies support the considering of canopy conditions and antenna placement when interpreting agricultural links, although their transmission distances and reception rates are dependent upon their respective settings.

Brief link disturbances close to the reception limit can produce isolated missing packets followed by successful reception. This is a plausible canopy-related explanation for a predominance of short episodes, consistent with the agricultural communication literature (Dai *et al*., 2024; Chapungo and Postolache, 2025; Alkhayyal and Mostafa, 2025). In this computational demonstration, however, the distribution establishes episode structure, rather than a physical cause. Furthermore, by themselves isolated episodes do not demonstrate statistical independence. The hourly calendar counts consecutive missed samples; it cannot resolve the precise beginning and end of a radio interruption.

Local storage plays a complementary role in this interpretation. In an implemented system, a reading retained locally but absent remotely can be distinguished from a reading that was never acquired. Also, the retaining of both acquisition and reception times separates delayed delivery from a true absence. These distinctions make the proposed workflow useful for investigating interruptions, without treating every remote gap as a sensor failure or assigning it automatically to the canopy.

5.3. Battery voltage and autonomy

The decline from 4.175 V in January to 3.823 V in December corresponds to a difference of 0.353 V between the unrounded monthly means. The annual range was 3.731–4.200 V. Every value therefore remains within the 3.0–4.2 V data-quality interval shown in Figure 2. This establishes consistency with the stated screening rule; however, the interval does not define the operating limits of the assembled node.

Battery-cell voltage and the regulated supply of the microcontroller describe different points in the power circuit. A deep-sleep function reduces consumption, but it does not establish a universal minimum battery voltage for the complete node. The regulator must supply the required output under the relevant load and temperature. Manufacturer specifications indicate that the input margin is dependent upon regulator dropout and operating conditions (Microchip Technology, 2022). These requirements concern the regulated supply under load; they cannot be inferred from the data-quality bounds alone.

The downward trend matters for multi-year operations because persistent discharge without sufficient replenishment would eventually threaten service. A year of voltage values within data-quality limits

does not establish that the regulated supply remains adequate through every operating state or across a period of several years. Furthermore, voltage decline alone does not determine a remaining lifetime in years. Such an estimate is dependent upon usable battery capacity, the measurement and transmission schedule, charging performance and their variation over time.

For solar-assisted monitoring, monthly means, minima and the timing of energy use should therefore be interpreted together. A monthly mean can conceal a lower value between charging periods, while a short period of adequate voltage does not describe the full annual cycle. Vieira *et al*. (2026) provide a useful field example for the reporting of delivery together with energy behavior in viticulture. The contribution of this study lies in the placing of the voltage profile beside the reception record, so that both can be examined over the same calendar, while retaining the distinction between a computational profile and demonstrated hardware autonomy.

5.4. Comparative evidence and transferability

Table 4 compares the workflow with agricultural monitoring systems and scientific loggers, identifying their evidence, functions and operating context.

LoRaFarM emphasizes a modular architecture for farm monitoring, while the irrigation system proposed by Froiz-Míguez *et al*. combines LoRa or LoRaWAN nodes with fog computing (Codeluppi *et al*., 2020; Froiz-Míguez *et al*., 2020). Dafonte *et al*. (2024) address calibrated soil-water monitoring in woody crops. While these studies illustrate how sensing and communication are assembled for particular agricultural purposes, the present workflow adds an explicit procedure for relating each scheduled observation to its origin, quality checks, reception status and energy context. This contribution concerns the organization and interpretation of records; the demonstration does not measure a performance improvement over those systems.

Vieira *et al*. (2026) report 1309 received messages out of 1345 expected messages, equivalent to 97.32%, during a 14-day field evaluation with a 15 min interval. Because the numerator, denominator and evaluation period are stated, their result provides a concrete reporting benchmark. The 95.0% reliability rate of our study describes 8322 records marked received out of 8760 scheduled hourly positions in a computational annual series. Differences in evidence, sampling interval, duration and power demand preclude a direct comparison of the two percentages as a controlled

Table 4. Technical positioning against selected agricultural systems and commercial scientific loggers

System	Sampling / evidence	Storage / power	Traceability / functions	Comparison scope
This workflow	60 min; computational 8760 h calendar	microSD design; 10 W solar; 3.7 V nominal cell	8322/8760 received; explicit missing states, calibration, events and quality rules	Demonstration of the reporting method
LoRaFarM (Codeluppi *et al*., 2020)	Modular farm/ vineyard deployment	Distributed sensing units	Modular sensing and middleware	Agricultural architecture; different evaluation
Froiz-Míguez *et al*. (2020)	Irrigation testbed; LoRa/LoRaWAN	Distributed sensing; fog/cloud services	Radio planning, sensing and irrigation integration	System implementation and empirical testing
Dafonte *et al*. (2024)	Proximal monitoring in woody crops	ESP32/LoRa; node/gateway memory	Probe calibration and configurable telemetry	Field soil-water monitoring
Ahmed *et al*. (2025)	Orchard; 915 MHz link tests	5-byte radio payload	Vegetation and spreading-factor effects	Short communication experiments
Xu *et al*. (2025)	Maize; 433 MHz trials	Variable antenna height	Propagation and obstruction effects	Different band and link geometry
Vieira *et al*. (2026)	14 d field evaluation; 15 min	Solar-assisted battery system	1309/1345 messages; 97.32% delivery	Different duration, load and evidence
CR310 (Campbell Scientific, 2026)	Programmable scan; maximum 10 Hz	30 MB flash; integrated 12 V battery solar-charge regulator	Programmable analog/digital, RS-232 and SDI-12 interfaces	Manufacturer specifications; no common field trial
RX3000 (Onset Computer Corporation, 2026)	Cellular models: 1 min–18 h logging	32 MB; 4 V, 10 Ah rechargeable lead-acid battery; solar compatible	Modular smart-sensor/cloud platform; NEMA 4X enclosure	Manufacturer specifications; configuration dependent

Note. Technical comparison, not a quality ranking or a common performance trial. Research results retain their stated sampling periods and evidence types. Commercial capabilities follow the cited manufacturer descriptions; RX3000 logging intervals refer to cellular models, and its NEMA 4X rating requires proper cable-channel installation. These specifications do not establish certification or equivalent performance for the proposed node.

DOI: 10.21142/SS-0702-2026-e178

comparison of reliability. Their useful common feature is a denominator tied to the acquisition schedule.

The orchard and maize experiments demonstrate why transferability involves more than choosing a radio module. Frequency, antenna height and vegetation conditions affect the link being evaluated (Ahmed *et al*., 2025; Xu *et al*., 2025). Similarly, manufacturer descriptions of scientific loggers establish available functions rather than performance within a shared agricultural trial. Table 3, therefore, supports comparison of design choices and reported evidence, without attributing a common test environment to the systems.

In practice, applying the workflow involves defining the expected calendar, preserving original readings and their origin, and recording acquisition and delivery separately. Calibration metadata then explain how readings were transformed, while event records provide temporal context. Estimated or completed values remain distinguishable during aggregation. Consequently, readers can compare expected and available observations, the distribution of gaps and the accompanying energy conditions across sites. While the demonstration establishes this reporting procedure, claims regarding yield, water savings or long-term field reliability require evidence of those outcomes.

6. Conclusions

The proposed workflow provides a reproducible way to interpret agricultural monitoring records by connecting the expected hourly calendar with data origin, quality checks, local acquisition, remote reception and battery voltage. Its main contribution is to preserve these relationships throughout processing, so that a missing remote record can be investigated in its acquisition and operating context.

The computational demonstration shows why several indicators are needed together. The 95.0% availability summarizes completeness, while the predominance of isolated episodes describes how the gaps are distributed. The positive annual difference between precipitation and reference evapotranspiration coexists with 235 days of a negative daily difference, illustrating the information lost through annual aggregation. The battery profile combines a decrease of 0.353 V in monthly mean voltage with a minimum of 3.731 V. Consistency with the data-quality interval describes the annual series and does not establish multi-year hardware autonomy.

Together, these procedures make monitoring reports easier to check and compare. Preserving the sampling schedule and data origin enables readers to assess the meaning of missing values and the scope of each indicator. This supports transfer of the workflow to other agricultural monitoring systems, with interpretation tied to the measurements and operating conditions documented for each application.

Data availability

An earlier version of the data and documentation is available via Mendeley Data (Carriazo-Regino *et al*., 2026; doi: 10.17632/9g6mrrd8yc.1).

Authors' contributions

Yulieth Carriazo-Regino: Conceptualization, methodology, investigation, data curation, validation, formal analysis, writing (original draft), writing (revision and editing).

Rubén Baena-Navarro: Conceptualization, methodology, software, data curation, formal analysis, visualization, writing (original draft), writing (revision and editing).

Mario Macea-Anaya: Methodology, validation, supervision, writing (revision and editing).

Research funding

This work was self-financed and received no external funding.

Conflicts of interest

The authors have no conflicts of interest to declare.

Ethical statement

This study employed environmental, soil, energy and telemetry data only; no personal data, sensitive information, biological samples, human participants or animal subjects were involved.

AI declaration

The authors declare that no artificial intelligence tool was used in any part of the manuscript preparation process.

Acknowledgments

Y. Carriazo-Regino, R. Baena-Navarro & M. Macea-Anaya express their gratitude to J. C. Emmanuel-Veritas, the Teacher of Living Wisdom, for the strength, clarity and guidance received during the development of this work. The authors also thank the Universidad de Córdoba and Universidad Americana de Europa (UNADE) for the academic and institutional support provided within the framework of this research.

Bibliographic references

Abdelmoneim, A. A., Al Kalaany, C. M., Khadra, R., Derardja, B., and Dragonetti, G. (2025). «Calibration of Low-Cost Capacitive Soil Moisture Sensors for Irrigation Management Applications». *Sensors*, 25(2), 343. Available at: https://www.mdpi.com/1424-8220/25/2/343

Ahmed, M. A., Gallardo, J. L., Zuniga, M. D., Pedraza, M. A., Carvajal, G., Jara, N., and Carvajal, R. (2022). «LoRa Based IoT Platform for Remote Monitoring of Large-Scale Agriculture Farms in Chile». *Sensors*, 22(8), 2824. Available at: https://www.mdpi.com/1424-8220/22/8/2824

Ahmed, S., Reza, M. N., Samsuzzaman, Karim, M. R., Jin, H., Kim, H., and Chung, S.-O. (2025). «Vegetation Effects on LoRa-Based Wireless Sensor Communication for Remote Monitoring of Automatic Orchard Irrigation Status». *IoT*, 6(1), 2. Available at: https://www.mdpi.com/2624-831X/6/1/2?utm_source=chatgpt.com

Aldhaheri, L., Alshehhi, N., Manzil, I. I. J., Khalil, R. A., Javaid, S., Saeed, N., and Alouini, M. S. (2025). «LoRa Communication for Agriculture 4.0: Opportunities, Challenges, and Future Directions». *IEEE Internet of Things Journal*, 12(2), pp. 1380-1407. Available at: https://ieeexplore.ieee.org/document/10735371

Alkhayyal, M. A., and Mostafa, A. M. (2025). «Enhancing LoRaWAN Performance Using Boosting Machine Learning Algorithms Under Environmental Variations». *Sensors*, 25(13), 4101. Available at: https://www.mdpi.com/1424-8220/25/13/4101

Allen, R. G., Pereira, L. S., Raes, D., and Smith, M. (1998). *Crop evapotranspiration: Guidelines for computing crop water requirements*. FAO Irrigation and Drainage Paper 56. Rome: Food and Agriculture Organization of the United Nations. Available at: https://www.fao.org/4/x0490e/x0490e00.htm

Analog Devices. (2019). «DS18B20: Programmable Resolution 1-Wire Digital Thermometer». Data Sheet Rev. 6. Available at: https://www.analog.com/en/products/ds18b20.html

Baena-Navarro, R., Torres-Hoyos, F., Uc-Rios, C., and Colmenares-Quintero, R. F. (2020). «Design and assembly of an IoT-based device to determine the absorbed dose of gamma and UV radiation». *Applied Radiation and Isotopes*, 166, 109359. Available at: https://www.sciencedirect.com/science/article/abs/pii/S0969804320305066

Baena-Navarro, R., Alcala-Varilla, L., Torres-Hoyos, F., Carriazo-Regino, Y., and Parodi-Camaño, T. (2024). «Gamma and ultraviolet radiation analysis: an internet of things-based dosimetric study». *Bulletin of Electrical Engineering and Informatics*, 13(5), pp. 3430-3445. Available at: https://beei.org/index.php/EEI/article/view/7344

Baena-Navarro, R., Carriazo-Regino, Y., and Macea-Anaya, M. (2026). «Interpretable artificial intelligence system for personalized cognitive stimulation». *IAES International Journal of Artificial Intelligence*, 15(1), pp. 164-176. Available at: https://ijai.iaescore.com/index.php/IJAI/article/view/29683

Barrios, C., Amaya, A., and Arce, D. (2025). «Digital Agroclimatic Plot: An open-field laboratory where technology and agriculture come together to transform farming». Alliance of Bioversity International and CIAT. Available at: https://alliancebioversityciat.org/publications-data/digital-agroclimatic-plot-open-field-laboratory-where-technology-and-agriculture

Bosch Sensortec. (2021). «BMP280 Digital Pressure Sensor: Technical specifications». Available at: https://www.bosch-sensortec.com/products/environmental-sensors/pressure-sensors/bmp280/

Bristow, N., Rengaraj, S., Chadwick, D. R., Kettle, J., and Jones, D. L. (2022). «Development of a LoRaWAN IoT Node with Ion-Selective Electrode Soil Nitrate Sensors for Precision Agriculture». *Sensors*, 22(23), 9100. Available at: https://www.mdpi.com/1424-8220/22/23/9100

Cadena-Torres, J., Novoa-Yáñez, R. S., Grandett-Martinez, L. M., Contreras-Santos, J. L., and Agamez-Saibis, A. (2021). *«Caracterización físico-química de los suelos dedicados al cultivo de maíz en el Valle del Sinú, Colombia». Temas Agrarios*, 26(1), pp. 68-79. Available at: https://revistas.unicordoba.edu.co/index.php/temasagrarios/article/view/2584

Campbell Scientific. (2026). «CR310. Measurement and Control Datalogger: Product specifications». Available at: https://www.campbellsci.com/products/cr310

Carriazo-Regino, Y., Baena-Navarro, R., and Macea-Anaya, M. (2026). «On-Site LoRaWAN IoT Dataset for Hydroclimatic and Soil Moisture Monitoring in Tropical Agriculture: Montería, Colombia, 2025». [dataset]. Mendeley Data, V1. Available at: https://data.mendeley.com/datasets/9g6mrrd8yc/1

Chapungo, N. J., and Postolache, O. (2025). «Experimental Evaluation of LoRaWAN Connectivity Reliability in Remote Rural Areas of Mozambique». *Sensors*, 25(19), 6027. Available at: https://www.mdpi.com/1424-8220/25/19/6027

Codeluppi, G., Cilfone, A., Davoli, L., and Ferrari, G. (2020). «LoRaFarM: A LoRaWAN-Based Smart Farming Modular IoT Architecture». *Sensors*, 20(7), 2028. Available at: https://www.mdpi.com/1424-8220/20/7/2028

Dafonte, J., González, M. Á., Comesaña, E., Teijeiro, M. T., and Cancela, J. J. (2024). «Soil Water Status Monitoring System with Proximal Low-Cost Sensors and LoRa Technology for Smart Water Irrigation in Woody Crops». *Sensors*, 24(24), 8104. Available at: https://www.mdpi.com/1424-8220/24/24/8104

Dai, Q., Chen, Z., Wu, G., Li, Z., Lv, S., and Huang, W. (2024). «LoRa Communication Quality Optimization on Agriculture Based on the PHY Anti-Frame Loss Mechanism». *Agriculture*, 14(3), 460. Available at: https://www.mdpi.com/2077-0472/14/3/460

Dhanaraju, M., Chenniappan, P., Ramalingam, K., Pazhanivelan, S., and Kaliaperumal, R. (2022). «Smart farming: Internet of Things (IoT)-based sustainable agriculture». *Agriculture*, 12(10), 1745. Available at: https://www.mdpi.com/2077-0472/12/10/1745

Froiz-Míguez, I., Lopez-Iturri, P., Fraga-Lamas, P., Celaya-Echarri, M., Blanco-Novoa, Ó., Azpilicueta, L., Falcone, F., and Fernández-Caramés, T. M. (2020). «Design, Implementation, and Empirical Validation of an IoT Smart Irrigation System for Fog Computing Applications Based on LoRa and LoRaWAN Sensor Nodes». *Sensors*, 20(23), 6865. Available at: https://www.mdpi.com/1424-8220/20/23/6865

García, L., Parra, L., Jimenez, J. M., Lloret, J., and Lorenz, P. (2020). «IoT-based smart irrigation systems: An overview on the recent trends on sensors and IoT systems for irrigation in precision agriculture». *Sensors*, 20(4), 1042. Available at: https://www.mdpi.com/1424-8220/20/4/1042

Loconsole, D., Elia, M., Conversa, G., De Lucia, B., Cristiano, G., and Elia, A. (2025). «Soil moisture sensing technologies: Principles, applications, and challenges in agriculture». *Agronomy*, 15(12), 2788. Available at: https://www.mdpi.com/2073-4395/15/12/2788

Mane, S., Das, N. N., Singh, G., Cosh, M. H., and Dong, Y. (2024). «Advancements in dielectric soil moisture sensor calibration: A comprehensive review of methods and techniques». *Computers and Electronics in Agriculture*, 218, 108686. Available at: https://www.sciencedirect.com/science/article/abs/pii/S0168169924000772

Microchip Technology. (2022). «MCP1825/MCP1825S. 500 mA, Low Voltage Low Quiescent Current LDO Regulator». Data sheet DS20002056C. Available at: https://ww1.microchip.com/downloads/aemDocuments/documents/APID/ProductDocuments/DataSheets/MCP1825-Family-Data-Sheet-DS20002056.pdf

Nsoh, B., Katimbo, A., Guo, H., Heeren, D. M., Nakabuye, H. N., Qiao, X., Ge, Y., Rudnick, D. R., Wanyama, J., Bwambale, E., and Kiraga, S. (2024). «Internet of Things-based automated solutions utilizing machine learning for smart and real-time irrigation management: A review». *Sensors*, 24(23), 7480. Available at: https://www.mdpi.com/1424-8220/24/23/7480

Obaideen, K., Yousef, B. A. A., AlMallahi, M. N., Tan, Y. C., Mahmoud, M., Jaber, H., and Ramadan, M. (2022). «An overview of smart irrigation systems using IoT». *Energy Nexus*, 7, 100124. Available at: https://www.sciencedirect.com/science/article/pii/S2772427122000791

Onset Computer Corporation. (2026). «HOBO RX3000 Remote Monitoring Station. Specifications». Available at: https://www.onsetcomp.com/products/data-loggers/rx3000

Pinedo-López, J., Baena-Navarro, R., Carriazo-Regino, Y., Torres-Hoyos, F., and Nieves-Garces, D. (2025). «Science, technology, and innovation policy and regional scientific production in Colombia: a methodological framework to address asymmetries in developing countries». *Journal of Innovation and Entrepreneurship*, 14, 89. Available at: https://link.springer.com/article/10.1186/s13731-025-00562-0

Raheja, A., Sharda, R., Garg, S., Kaur, S., Das, S., and Choudhary, O. P. (2025). «Designing and field calibration of low-cost microcontroller-based soil moisture sensor for subsurface drip-irrigation system». *Scientific Reports*, 15, 35948. Available at: https://www.nature.com/articles/s41598-024-81288-z

TE Connectivity. (2017). «HTU21D Digital High Accuracy RH/T Sensor. Product specifications». Available at: https://www.te.com/en/product-CAT-HSC0004.html

***Unidad de Planificación Rural Agropecuaria* (UPRA). (2025).** *Identificación de las zonas de protección para la producción de alimentos (ZPPA) en el departamento de Córdoba*. Bogotá: UPRA. Available at: https://upra.gov.co/en/node/2028

Vidal-Durango, J., Baena-Navarro, R., and Therán-Nieto, K. (2024). «Implementation and feasibility of green hydrogen in Colombian kitchens: an analysis of innovation and sustainability». *Indonesian Journal of Electrical Engineering and Computer Science*, 34(2), pp. 726-744. Available at: https://repositorio.cuc.edu.co/entities/publication/0e07bb96-2d20-4ef9-9c95-4f9b036c14ff

Vieira, A., Silva, N., Pascoal, D., and Morais, R. (2026). «A Versatile and Low-Cost IoT Solution for Bioclimatic Monitoring in Precision Viticulture». *Future Internet*, 18(1), 16. Available at: https://www.mdpi.com/1999-5903/18/1/16

World Meteorological Organization. (2018). Guide to Instruments and Methods of Observation. Volume I: Measurement of Meteorological Variables. WMO-No. 8. Geneva: World Meteorological Organization. Available at: https://community.wmo.int/site/knowledge-hub/programmes-and-initiatives/instruments-and-methods-of-observation-programme-imop/guide-instruments-and-methods-of-observation-wmo-no-8-0

Xu, T., Ma, D., Fang, W., and Huang, Y. (2025). «Experimental Study on the Propagation Characteristics of LoRa Signals in Maize Fields». *Electronics*, 14(11), 2156. Available at: https://www.mdpi.com/2079-9292/14/11/2156

Zhang, H., He, L., Di Gioia, F., Choi, D., Elia, A., and Heinemann, P. (2022). «LoRaWAN based internet of things (IoT) system for precision irrigation in plasticulture fresh-market tomato». *Smart Agricultural Technology*, 2, 100053. Available at: https://www.sciencedirect.com/science/article/pii/S2772375522000181